

## NUMERICAL OPTIMIZATION OF THE CANTILEVER PIEZOELECTRIC GENERATOR

A.N. Soloviev<sup>1,2</sup>, V.A. Chebanenko<sup>3\*</sup>, I.V. Zhilyaev<sup>4</sup>, A.V. Cherpakov<sup>1,2</sup>, I.A. Parinov<sup>2</sup>

<sup>1</sup>Don State Technical University, Gagarin sq. 1, Rostov-on-Don, Russia

<sup>2</sup>Vorovich Mathematics, Mechanics and Computer Science Institute, Southern Federal University,  
Milchakova st., 8a, Rostov-on-Don, Russia

<sup>3</sup>Federal Research Center "Southern Scientific Center of the Russian Academy of Sciences", Chekhova st., 41,  
Rostov-on-Don, Russia

<sup>4</sup>University of Applied Sciences and Arts Northwestern Switzerland, Institute of Polymer Engineering,  
Bahnhofstrasse, 6, Windisch, Switzerland

\*e-mail: valera.chebanenko@yandex.ru

**Abstract.** In this paper, we consider the adequacy of the use of the straight normal hypothesis in the applied theory for the calculation of a cantilever-type piezoelectric generator that takes into account the incomplete piezo-element coating of the substrate, which was obtained earlier, and a numerical optimization procedure for piezoelectric generator is given, taking into account critical failure stresses.

**Keywords:** piezoelectric generator, banding, straight normal, semi-analytical method, finite element, numerical optimization

### 1. Introduction

It is known that piezoelectric materials are widely used as actuators, sensors and generators in the engineering and aerospace field for monitoring the state of structures, shape control, active suppression of parasitic vibrations, noise suppression, etc. Such wide application is achieved due to their good electromechanical properties, flexibility in the design process, ease of production, as well as high energy conversion efficiency in the direct and inverse piezo effect. When using piezoelectric materials as actuators, deformations can be controlled by changing the magnitude of the applied electric potential. In the sensors, deformation measurement is also performed by measuring the induced potential. In the field of energy harvesting by means of piezoelectric materials, the free mechanical energy that is present in the environment is converted into electrical, and then converted into a suitable for low-power device. A detailed survey is given in [1-3]

In recent years, research has been actively developed in the area of piezoelectric transducers of mechanical energy into electrical one. This type of transducers was called piezoelectric generators (PEG). The basic information about PEG, as well as the problems arising at the development stages of energy storage devices, were given in the review papers [3-5], as well as in the fundamental monograph [6].

Typical actuators, sensors and generators, working on bending, are a multi-layered structure consisting of several layers with different mechanical and electrical properties. The traditional design, consisting of two piezoelectric layers, glued to the substrate or to each other is called a bimorph.

Most of the works are devoted to the study of the characteristics of the bimorph cantilever type PEG. There are several ways of modeling PEG: mathematical model with lumped parameters, mathematical model with distributed and finite element (FE) model.

Works [7-9] are devoted to the construction of PEG models on the basis of oscillations of a mechanical system with lumped parameters. The use of such systems is a convenient model approach, since it allows obtaining analytical dependencies between the output parameters of PEG (potential, power, etc.) and electrical, mechanical characteristics and resistance of the external electric circuit.

Simulation using lumped parameters gives an initial idea of the problem, allowing simple expressions to be used to describe the system. However, this simulation method is inaccurate and limited to only one mode of oscillation. In addition, the approach does not take into account important aspects of the related physical system, for example, information on the dynamic form of the oscillation mode and accurate information on the distribution of deformation and its effect on the electrical response of the system.

Another type of simulation is modeling using distributed parameters. Based on the Euler-Bernoulli hypotheses for a beam, analytic solutions of the related problem were obtained in [10,11] for various configurations of the cantilever type PEG. Explicit expressions for the output voltage across the resistor for harmonic oscillations of the cantilever beam were obtained. In addition, the authors studied in detail the behavior of PEG with short-circuited and open-circuit electrical circuits and the effect of the electromechanical coupling coefficient. However, in these studies, the case where the piezoelectric element (PE) does not completely cover the substrate has not been considered.

Works [11-14] are devoted to the FE modeling of cantilever PEGs of various configurations. The case where the PE does not completely cover the substrate is also easily solved by the FE method. Nevertheless, obtaining a numerical-analytical solution for the case of incomplete coating of the substrate by a PE is of some interest.

The above brief analysis of known works has shown that the problem of modeling PEG using analytical methods in full is not yet solved, although it is very relevant.

In previous works, we presented a numerical analytical model based on the Kantorovich method [15], confirmed by FE modeling and a series of experiments [16], and also carried out a FE analysis of the improved model of cantilever PEG [17].

In this paper, we consider the adequacy of the use of the straight normal hypothesis in the applied theory for the calculation of a cantilever-type PEG that takes into account the incomplete PE coating of the substrate, which was obtained earlier in [15], and a numerical optimization procedure for PEG is given, taking into account critical failure stresses.

## 2. Mathematical modelling of the cantilever PEG

The simplest bimorph design of cantilever PEG is presented in Fig. 1. The cantilever bimorph PEG consists of two PEs (Fig. 1, points 1 and 3) glued to the substrate (Fig. 1, point 2), which is clamped from one end. Electrodes are applied to large sides perpendicular to the  $x_3$  axis. The electrical voltage  $v(t)$  is measured on the resistor  $R$ .

Piezoelectric elements are polarized in thickness. In this paper, we consider a parallel circuit for connecting PEs to a common electric circuit (see Fig. 1); therefore, it is assumed that the polarization vectors are aligned with the positive direction of the  $x_3$  axis.

The excitation of oscillations in the PEG shown in Fig. 1 occurs through the movement of the clamp relative to a certain plane, so the absolute displacement of the cantilever along the coordinate  $x_3$  will consist of the displacement of the clamp  $w_c(t)$  and the relative displacement of the cantilever  $w(x_1, t)$ .

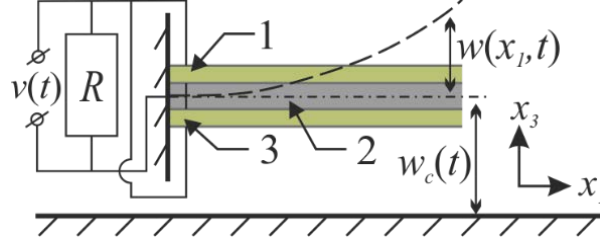


**Fig. 1.** Bimorph cantilever PEG: 1 and 3 - PEs, 2 - substrate

To analyze the problem of forced oscillations of a cantilever bimorph PEG in [15], we used the Kantorovich method [18]. It is based on the idea of the expansion of the displacement of the beam in a row:

$$w(x_1, t) = \sum_{i=1}^N \eta_i(t) \phi_i(x_1), \quad (1)$$

where  $N$  is the number of vibration modes to be considered,  $\eta_i(t)$  is unknown generalized coordinates,  $\phi_i(x_1)$  are known test functions that satisfy the boundary conditions.

Earlier, in [15], applied numerical theories were constructed to simulate the performance characteristics of a cantilever type PEG. Simulation took place on the basis of the Hamilton principle within the framework of the Euler-Bernoulli hypotheses:

$$\begin{aligned} \mathbf{M}\ddot{\boldsymbol{\eta}}(t) + \mathbf{D}\dot{\boldsymbol{\eta}}(t) + \mathbf{K}\boldsymbol{\eta}(t) - \boldsymbol{\Theta}v(t) &= \mathbf{p}, \\ C_p \dot{v}(t) + \boldsymbol{\Theta}^T \dot{\boldsymbol{\eta}}(t) + \frac{v(t)}{R} &= 0, \end{aligned} \quad (2)$$

where  $\mathbf{D} = \mu\mathbf{M} + \gamma\mathbf{K}$  is the Rayleigh-type damping matrix, and the remaining coefficients are:

$$\begin{aligned} C_p &= \frac{b_p L_p}{h_p} \mathfrak{e}_{33}^{S*}, & K_{ij} &= \int_0^L EI \phi_i''(x_1) \phi_j''(x_1) dx_1, & \theta_i &= \int_0^L J_p \phi_i''(x_1) dx_1, \\ M_{ij} &= \int_0^L m \phi_i(x_1) \phi_j(x_1) dx_1, & p_i &= -\ddot{w}_c(t) \left[ \int_0^L m \phi_i(x_1) dx_1 \right], \end{aligned} \quad (3)$$

where  $M_{ij}$  is the elements of the mass matrix,  $K_{ij}$  is the elements of the stiffness matrix,  $v(t)$  is the voltage across the resistor  $R$ ,  $C_p$  is the electrical capacitance,  $\theta_i$  is the elements of the electromechanical coupling vector,  $p_i$  is elements of the effective mechanical load vector.

Next we will consider PEG, the substrate of which has the following characteristics: geometric dimensions  $L \times b \times h$ ,  $108 \times 10 \times 1$  mm<sup>3</sup>, density  $\rho_s$  1650 kg/m<sup>3</sup>, elastic modulus  $c_s$  15 GPa. PEs have the following characteristics: geometric dimensions  $L_p \times b_p \times h_p$ ,  $56 \times 6 \times 0.5$  mm<sup>3</sup>, density  $\rho_p$  8000 kg/m<sup>3</sup>, elastic modulus  $c_p$  7.5 GPa, relative permittivity  $\epsilon_{33}^S / \epsilon_0$  5000, piezoelectric modulus  $d_{31}$  350 pC/N. The excitation in the system is given by the harmonic displacement of the base  $w_c = \tilde{w}_c e^{i\omega t}$ , whose amplitude is  $\tilde{w}_c = 0.1$  mm.

The damping coefficients  $\mu$  and  $\gamma$  for the natural frequencies  $\omega_i$  and  $\omega_j$  are found from the solution of the following equation [19]:

$$\frac{1}{2} \begin{bmatrix} 1/\omega_i & \omega_i \\ 1/\omega_j & \omega_j \end{bmatrix} \begin{Bmatrix} \mu \\ \gamma \end{Bmatrix} = \begin{Bmatrix} \xi_1 \\ \xi_2 \end{Bmatrix}, \quad (4)$$

where  $\xi_1$  and  $\xi_2$  are the modal damping coefficients, which are selected for reasons of agreement with the experimental data. In this work, the modal damping coefficients for the first two modes were set equal to  $\xi_1 = \xi_2 = 0.02$  in accordance with the results of earlier experimental studies of cantilever PEGs [16].

### 3. Adequacy of the hypothesis of a straight normal

The Euler-Bernoulli hypotheses assume that the beam is uniform in thickness. In our case, we have a three-layer beam (Fig. 2). Moreover, the modulus of elasticity of the substrate (inner layer) is 3.8 times smaller than the elastic modulus of the PEs (outer layers). This fact may indicate a break in the normal when the beam is bent. This in turn can lead to inaccurate results when using the theory based on the Euler-Bernoulli hypotheses in the calculation of such a construction. With the help of the FE calculation, we analyze the deformations in the cross section of the beam and compare them with theory.

For the analysis, a model of cantilever bimorph PEG, shown in Fig. 2, was chosen.

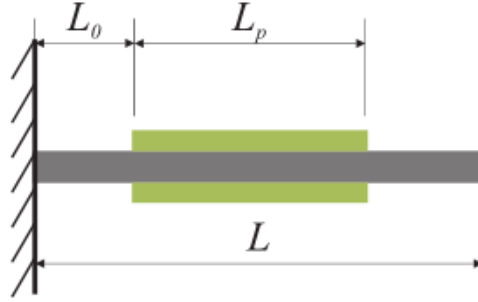


Fig. 2. Cantilever type PEG

In order to take into account the incomplete covering of the piezoelectric substrate by the generator shown in Fig. 2, the function  $\phi_i(x_1)$  should be specified as follows:

$$\phi_i(x_1) = \begin{cases} \phi_i^{(1)}(x_1), & x_1 \leq L_0 \\ \phi_i^{(2)}(x_1), & L_0 < x_1 \leq L_0 + L_p \\ \phi_i^{(3)}(x_1), & x_1 > L_0 + L_p \end{cases} \quad (5)$$

In this case, the specific mass  $m$ , for the cross section shown in Fig. 2, is calculated as follows:

$$m = \rho_s S_s + 2\rho_p S_p, \quad (6)$$

where  $\rho_s$  is the density of the substrate,  $\rho_p$  is the piezoceramic density,  $S_s = hb$  is the cross-sectional area of the substrate, and  $S_p = h_p b_p$  is the cross-sectional area of the PE.

The flexural rigidity  $EI$  for this construction is calculated as follows:

$$EI = c_p \left[ \iint_{S_{pup}} x_3^2 dS + \iint_{S_{plow}} x_3^2 dS \right] + c_s \iint_{S_s} x_3^2 dS, \quad (7)$$

where  $c_p$  and  $c_s$  are the moduli of elasticity of piezoceramics and substrates, respectively, and  $S_{pup}$  and  $S_{plow}$  are the cross-sectional areas along which integration is performed for the lower and upper PEs, respectively.

The function  $J_p$  in the electromechanical coupling vector is:

$$J_p = \frac{e_{31}^*}{h_p} \left( \iint_{S_{pup}} x_3 dS + \iint_{S_{plow}} x_3 dS \right). \quad (8)$$

The boundary conditions and the conjugation conditions necessary for finding the functions  $\phi_i(x_1)$  for a given construction will be as follows:

$$\begin{aligned}
\phi_i^{(1)}(0) &= 0, & \phi_i^{(2)'''}(L_0 + L_p) &= \frac{EI^{(1)}}{EI^{(2)}} \phi_i^{(3)'''}(L_0 + L_p), \\
\phi_i^{(1)'}(0) &= 0, & \phi_i^{(2)''''}(L_0 + L_p) &= \frac{EI^{(1)}}{EI^{(2)}} \phi_i^{(3)''''}(L_0 + L_p), \\
\phi_i^{(1)}(L_0) &= \phi_i^{(2)}(L_0), & \phi_i^{(2)}(L_0 + L_p) &= \phi_i^{(3)}(L_0 + L_p), \\
\phi_i^{(1)'}(L_0) &= \phi_i^{(2)'}(L_0), & \phi_i^{(2)'}(L_0 + L_p) &= \phi_i^{(3)'}(L_0 + L_p), \\
\phi_i^{(1)''}(L_0) &= \frac{EI^{(2)}}{EI^{(1)}} \phi_i^{(2)''}(L_0), & \phi_i^{(3)''}(L) &= 0, \\
\phi_i^{(1)'''}(L_0) &= \frac{EI^{(2)}}{EI^{(1)}} \phi_i^{(2)'''}(L_0), & \phi_i^{(3)'''}(L) &= 0,
\end{aligned} \tag{9}$$

where  $EI^{(1)}$  is the bending stiffness of the segment without a PE, and  $EI^{(2)}$  with a PE.

A similar problem was modeled in the ACELAN FE package. With a certain indentation to the right at three points near the left edge of the PE, the longitudinal strain distributions along the thickness were obtained (see Fig. 3).

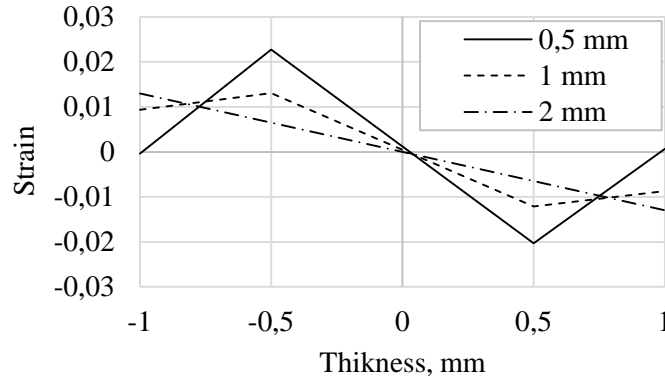


**Fig. 3.** Strain distribution along the thickness in the vicinity of the left edge of PE

The FE calculation showed that, in the vicinity of the first resonance frequency, the deflected mode of the three-layer structure is well described by the hypothesis of a single normal, with the exception of the edges of the PE, and the size of this region does not exceed the thickness of the packet. Thus, in Fig. 3, the plots of the longitudinal strain distribution along the beam thickness for distances from the left edge of the PE 0.5, 1 and 2 mm are shown for the model shown in Fig. 2. A similar distribution is also found at the right edge of the PE. Considering that the PE length in calculation is 56 mm, the applied theory of oscillations of a three-layer beam is described with a high degree of accuracy on the basis of the hypothesis of a single normal.

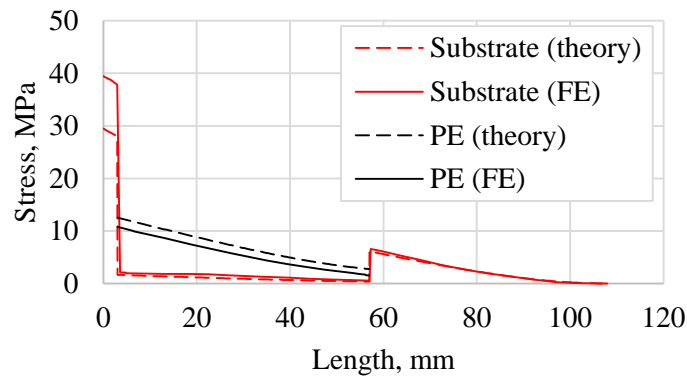


**Fig 4.** Stress distribution in the cantilever transducer along the length of transducer on the upper surfaces of layers

Comparison of the results of the calculation of the stress-strain and electric state of cantilever transducer according to the applied theory and the FE model in the framework of the deflected mode with the condition of an open circuit at a frequency in the neighborhood of the first resonance shows a good qualitative coincidence of the characteristics (Fig. 4 and 5). In quantitative terms, with a relative deflection difference of 9%, the relative difference in maximum stresses at the free boundaries of the PE in their middle part along the length did not exceed 10%. In addition, a comparison was made with the known FE model, built in the ANSYS package, according to which the relative error in determining the resonant frequencies and the output electric voltage was 6%.

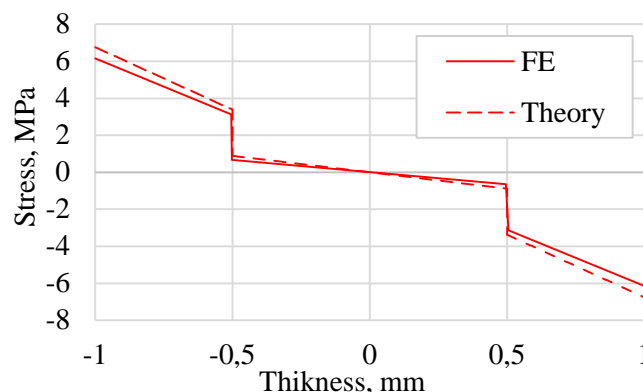


**Fig 5.** Stress distribution in the cantilever transducer along the thickness in the middle point of PE

#### 4. Numerical optimization

Of particular interest is the study of the influence of geometric parameters on the output characteristics of PEG, taking into account the critical stresses for each material. We introduce the strength limit in the following form

$$\sigma_m = k\sigma_c, \quad (10)$$

here,  $\sigma_m$  is the maximum permissible value of the mechanical stress,  $k$  is the safety factor, and  $\sigma_c$  is the critical value of the mechanical stress at which the material is broken.

For substrate and PE materials [20], let us take the critical values of  $\sigma_c$  for the case of tension equal to 150 and 66 MPa, respectively. Safety factor is  $k = 0.5$ .

For optimization, a bimorph cantilever PEG model with an attached mass, which is located at some margin on the free end of the beam, was selected (see Fig. 6.).

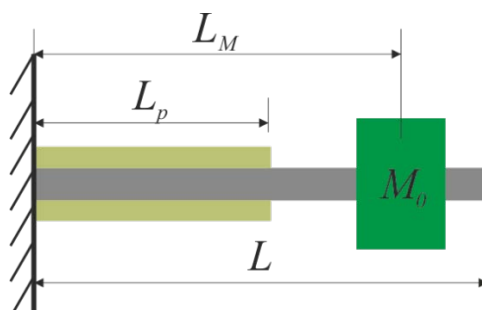


**Fig. 6.** Cantilever type PEG with proof mass

In order to take into account the incomplete covering of the piezoelectric substrate by the generator shown in Fig. 6, the function  $\phi_i(x_1)$  should be given as follows:

$$\phi_i(x_1) = \begin{cases} \phi_i^{(1)}(x_1), & x_1 \leq L_p \\ \phi_i^{(2)}(x_1), & L_p < x_1 \leq L_M \\ \phi_i^{(3)}(x_1), & x_1 > L_M \end{cases} \quad (11)$$

Adding an attached mass to the design requires consideration of its influence in the system of differential equations, since it is an additional inertial load that affects the kinetic energy. Taking into account the attached mass, the expressions for the components  $M_{ij}$  and  $p_i$  vary as follows:

$$M_{ij} = \int_0^L m\phi_i(x_1)\phi_j(x_1)dx_1 + M_0\phi_i(L_M)\phi_j(L_M), \quad (12)$$

$$p_i = -\ddot{w}_c(t) \int_0^L m\phi_i(x_1)dx_1 + M_0\phi_i(L_M),$$

where  $L_M$  is the position coordinate of the attached mass. In this case it is the free end of the beam.

The boundary conditions and the conjugation conditions for finding  $\phi_i(x_1)$  will be as follows:

$$\begin{aligned} \phi_i^{(1)}(0) &= 0, & \phi_i^{(2)''}(L_M) &= \phi_i^{(3)''}(L_M), \\ \phi_i^{(1)'}(0) &= 0, & \phi_i^{(2)''''}(L_M) &= \phi_i^{(3)''''}(L_M) - \alpha\beta^4\phi_i^{(2)}(L_M), \\ \phi_i^{(1)}(L_p) &= \phi_i^{(2)}(L_p), & \phi_i^{(2)}(L_M) &= \phi_i^{(3)}(L_M), \\ \phi_i^{(1)'}(L_p) &= \phi_i^{(2)'}(L_p), & \phi_i^{(2)'}(L_M) &= \phi_i^{(3)'}(L_M), \\ \phi_i^{(1)''}(L_p) &= \frac{EI^{(2)}}{EI^{(1)}}\phi_i^{(2)''}(L_p), & \phi_i^{(3)''}(L) &= 0, \\ \phi_i^{(1)''''}(L_p) &= \frac{EI^{(2)}}{EI^{(1)}}\phi_i^{(2)''''}(L_p), & \phi_i^{(3)''''}(L) &= 0, \end{aligned} \quad (13)$$

where  $\alpha = M / mL$ ,  $\beta$  is an eigenvalue,  $EI^{(1)}$  is the bending stiffness of a segment covered by a PE, and  $EI^{(2)}$  is without a PE.

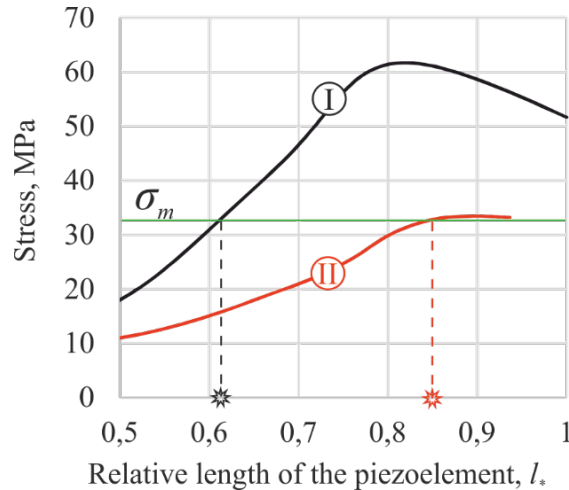


**Fig 7.** Dependences of the maximum mechanical stresses arising in the clamp of PEG on the relative length  $l_*$  of PE for two configurations

Investigations of the efficiency of various types of structures from geometric parameters with allowance for the critical tensile stresses for a piezoceramic layer and a substrate are carried out. Thus, for the model shown in Fig. 6, the dependence of the output parameters on the PE's length was compared in the presence of (I) and the absence (II) of the attached mass  $M_0$ .

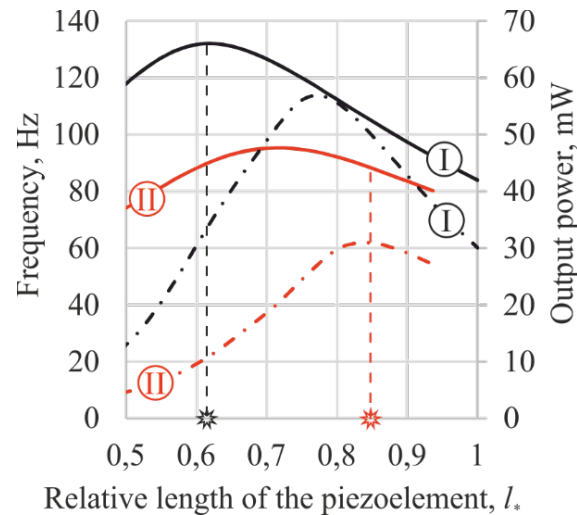


**Fig. 8.** Dependences of the output parameters of PEG on the relative length  $l_*$  of PE for two configurations: resonance frequencies (solid lines) and maximum output power (dot-dash lines)

The results of the research showed that, in the presence and absence of  $M_0$ , mechanical stresses begin to exceed the permissible stress limits  $\sigma_m$  beginning with a certain value of the PE's length (see Fig. 7). It turned out that there is an interval of frequencies (82-94 Hz) where the first resonance frequencies in the case of the presence (I) and absence (II) of the attached mass coincide. The maximum power that can be obtained in the presence of  $M_0$  (I) was about 31 mW at a frequency of 88 Hz with the relative length of PE  $l_* = L_p / L_0$  equal to 0.85 (see Fig. 8). The same output power can be obtained in the absence of  $M_0$  (II) at a frequency of 131 Hz for a length  $l_* = 0.63$ .

## 5. Conclusions

It is shown that the developed applied theory based on the single normal hypothesis satisfactorily describes the deflected mode in the internal part of the PEs. An exception to this is the small vicinity of the ends of piezoelectric layers, but the effect of this feature on the integral characteristics of piezoelectric is not significant.

An example of optimization of a cantilever-type PEG is shown taking into account the critical mechanical stresses for PEG materials. The optimization results showed that there is a frequency interval where the first resonant frequencies of the PEG with the attached mass and without coincide, but the PEG model without the presence of mass can not work in this interval, since the threshold of critical stresses is exceeded.

**Acknowledgements.** The publication was prepared in the framework of RFBR grant № 18-38-00912 mol\_a.

## References

- [1] Gaudenzi P. *Smart structures: physical behavior, mathematical modeling and applications*. New York: Wiley; 2009.
- [2] Chopra I. Review of state of art of smart structures and integrated systems. *AIAA Journal*. 2002;40(11): 2145-2187.
- [3] Chebanenko VA, Akopyan VA, Parinov IA. Piezoelectric generators and energy harvesters: modern state of the art. In: Parinov IA (ed.) *Piezoelectrics and Nanomaterials: Fundamentals, Developments and Applications*. New York: Nova Science Publishers; 2015. p.243-277.

- [4] Liu Y, Tian G, Wang Y, Lin J, Zhang Q, Hofmann HF. Active piezoelectric energy harvesting: general principle and experimental demonstration. *Journal of Intelligent Material Systems and Structures*. 2009;20(5): 575-586.
- [5] Liao Y, Sodano HA. Structural effects and energy conversion efficiency of power harvesting. *Journal of Intelligent Material Systems and Structures*. 2009;20(5): 505-515.
- [6] Erturk A, Daniel JI. *Piezoelectric energy harvesting*. New York: John Wiley & Sons; 2011.
- [7] Dutoit NE, Brian LW, Kim SG. Design considerations for MEMS-scale piezoelectric mechanical vibration energy harvesters. *Integrated Ferroelectrics*. 2005;71(1): 121-160.
- [8] Adhikari S, Friswell MI, Inman DJ. Piezoelectric energy harvesting from broadband random vibrations. *Smart Materials and Structures*. 2009;18(11): 115005.
- [9] Shu YC, Lien IC. Analysis of power output for piezoelectric energy harvesting systems. *Smart materials and structures*. 2006;15(6): 1499.
- [10] Erturk A, Inman DJ. On mechanical modeling of cantilevered piezoelectric vibration energy harvesters. *Journal of Intelligent Material Systems and Structures*. 2008;19(11): 1311-1325.
- [11] Stanton SC, McGehee CC, Mann BP. Nonlinear dynamics for broadband energy harvesting: Investigation of a bistable piezoelectric inertial generator. *Physica D: Nonlinear Phenomena*. 2010;239(10): 640-53.
- [12] Nechibvute A, Chawanda A, Luhanga P. Finite element modeling of a piezoelectric composite beam and comparative performance study of piezoelectric materials for voltage generation. *ISRN Materials Science*. 2012;2012: 1-11.
- [13] Solovyev AN, Duong LV. Optimization for the harvesting structure of the piezoelectric bimorph energy harvesters circular plate by reduced order finite element analysis. *International Journal of Applied Mechanics*. 2016;8(3): 1650029.
- [14] Junior CD, Erturk A, Inman DJ. An electromechanical finite element model for piezoelectric energy harvester plates. *Journal of Sound and Vibration*. 2009;327(1-2): 9-25.
- [15] Soloviev AN, Chebanenko VA, Parinov IA. Mathematical modelling of piezoelectric generators on the base of the Kantorovich method. In: *Analysis and Modelling of Advanced Structures and Smart Systems*. Singapore: Springer; 2018. p.227-258.
- [16] Shevtsov SN, Soloviev AN, Parinov IA, Cherpakov AV, Chebanenko VA. *Piezoelectric Actuators and Generators for Energy Harvesting*. Heidelberg: Springer; 2018.
- [17] Soloviev AN, Parinov IA, Cherpakov AV, Chebanenko VA, Rozhkov EV. Analyzing the output characteristics of a double-console PEG based on numerical simulation. *Materials Physics and Mechanics*. 2018;37(2): 168-175.
- [18] Wait R, Mitchell AR. *Finite element analysis and applications*. New York: John Wiley & Sons Inc; 1985.
- [19] Chopra AK. *Dynamics of structures. Theory and Applications to Earthquake Engineering*. New Jersey: Prentice Hall; 2017.
- [20] Zatsarinniy VP. *Strength of piezoceramics*. Rostov-on-Don: Publishing house of Rostov State University; 1978. (In Russian)